




# Naringenin mitigates titanium dioxide (TiO<sub>2</sub>)-induced chronic arthritis in mice: role of oxidative stress, cytokines, and NFκB

Marília F. Manchope<sup>1</sup> · Nayara A. Artero<sup>2</sup> · Victor Fattori<sup>1</sup> · Sandra S. Mizokami<sup>1</sup> · Dimitrius L. Pitol<sup>3</sup> · João P. M. Issa<sup>3</sup> · Sandra Y. Fukada<sup>4</sup> · Thiago M. Cunha<sup>5</sup> · José C. Alves-Filho<sup>5</sup> · Fernando Q. Cunha<sup>5</sup> · Rubia Casagrande<sup>2</sup> · Waldiceu A. Verri Jr.<sup>1</sup> 

Received: 5 March 2018 / Revised: 14 September 2018 / Accepted: 12 October 2018 / Published online: 28 October 2018  
© Springer Nature Switzerland AG 2018

## Abstract

**Objective** To evaluate the effect and mechanisms of naringenin in TiO<sub>2</sub>-induced chronic arthritis in mice, a model resembling prosthesis and implant inflammation.

**Treatment** Flavonoids are antioxidant and anti-inflammatory molecules with important anti-inflammatory effect. Mice were daily treated with the flavonoid naringenin (16.7–150 mg/kg, orally) for 30 days starting 24 h after intra-articular knee injection of 3 mg of TiO<sub>2</sub>.

**Methods** TiO<sub>2</sub>-induced arthritis resembles cases of aseptic inflammation induced by prosthesis and/or implants. Mice were stimulated with 3 mg of TiO<sub>2</sub> and after 24 h mice started to be treated with naringenin. The disease phenotype, treatment toxicity, histopathological damage, oxidative stress, cytokine expression and NFκB were evaluated after 30 days of treatment.

**Results** Naringenin inhibited TiO<sub>2</sub>-induced mechanical hyperalgesia (96%), edema (77%) and leukocyte recruitment (74%) without inducing toxicity. Naringenin inhibited histopathological index (HE, 49%), cartilage damage (Toluidine blue tibial staining 49%, and proteoglycan 98%), and bone resorption (TRAP-stained 73%). These effects were accompanied by inhibition of oxidative stress (gp91<sup>phox</sup> 93%, NBT 83%, and TBARS 41%) cytokine mRNA expression (IL-33 82%, TNFα 76%, pro-IL-1β 100%, and IL-6 61%), and NFκB activation (100%).

**Conclusion** Naringenin ameliorates TiO<sub>2</sub>-induced chronic arthritis inducing analgesic and anti-inflammatory responses with improvement in the histopathological index, cartilage damage, and bone resorption.

**Keywords** Flavonoids · Arthritis · Implant · Arthroplasty · Pain · Aseptic inflammation

## Introduction

Arthroplasty is a successful procedure in advanced cases of inflammatory arthritis including osteoarthritis and rheumatoid arthritis, and also in cases of fractures and osteonecrosis that replaces the dysfunctional joint for a prosthesis [1,

2]. Exemplifying the importance of this procedure, nearly 7 million Americans had total knee or hip replacements in 2010 and until 2030 close to 11 millions of Americans will have total knee or hip replacements [3]. In this sense, arthroplasty is an efficient and successful procedure with a low relative cost for terminal stage patients with dysfunctional joints [4]. Despite the success of the arthroplasty procedure,

Responsible Editor: Jason J. McDougall.

✉ Waldiceu A. Verri Jr.  
waverr@uel.br; waldiceujr@yahoo.com.br

<sup>1</sup> Present Address: Departamento de Ciências Patológicas, Centro de Ciências Biológicas, Universidade Estadual de Londrina, Rod. Celso Garcia Cid Km480 PR445, Cx Postal 10.011, Londrina, Paraná CEP 86057-970, Brazil

<sup>2</sup> Departamento de Ciências Farmacêuticas, Centro de Ciências de Saúde, Universidade Estadual de Londrina, Londrina, Brazil

<sup>3</sup> Departamento de Morfologia, Fisiologia e Patologia Básica, Faculdade de Odontologia de Ribeirão Preto, Universidade de São Paulo, Ribeirão Preto, São Paulo, Brazil

<sup>4</sup> Departamento de Física e Química, Faculdade de Ciências Farmacêuticas de Ribeirão Preto, Universidade de São Paulo, Ribeirão Preto, São Paulo, Brazil

<sup>5</sup> Departamento de Farmacologia, Faculdade de Medicina de Ribeirão Preto, Universidade de São Paulo, Ribeirão Preto, São Paulo, Brazil

about 10–15% of the patients present osteolysis and failure in prosthesis-replaced dysfunctional joint due to immune-inflammatory [5] response to debris biomaterials of the prosthesis released by wearing [6].

The titanium dioxide (TiO<sub>2</sub>) is a white and odorless powder used in designing prosthesis and implants in orthopedic and dentistry fields [7, 8]. There is evidence that TiO<sub>2</sub> is a contributing molecule to prosthesis or implants wear debris-induced inflammation. In agreement with the rationale that implants induce inflammation, a patient without a familiar history of rheumatic diseases developed implant-related arthritis due to titanium translocation from the cervical cage implant to the joints [9]. Furthermore, incubation of TiO<sub>2</sub> with patient's peripheral mononuclear blood cells induces TNF $\alpha$  release [9]. TiO<sub>2</sub>-induced chronic arthritis is a useful model in translational medicine to study the cellular and molecular mechanisms that involve TiO<sub>2</sub>-triggered chronic joint inflammation and bone destruction. In fact, TiO<sub>2</sub> induces articular pain, knee edema, oxidative stress, IL-33, TNF $\alpha$ , IL-1 $\beta$ , and IL-6 inflammatory cytokines production, and increased RANKL/RANK signaling pathway ultimately leading to joint destruction [10].

The flavonoid naringenin (4',5,7-trihydroxy-flavanone) is a polyphenol compound found in the human diet [11], mainly in citrus fruits including lemon, orange, tangerine, and grapefruit [12]. Mice oral intake of 200 mg of a Chinese extract containing naringenin is absorbed and plasma concentration is detected in 60 min. The elimination half-life of naringenin is 4.69 h and its elimination is almost complete in 24 h [13]. Regarding naringenin pharmacological activities, this flavonoid is an analgesic molecule [14–16] acting through the activation of the analgesic signalling pathway NO–cGMP–PKG–K<sub>ATP</sub> channel [14]. In addition to its analgesic action, naringenin reveals anti-inflammatory activity by inhibiting TNF $\alpha$  [14, 15], IL-1 $\beta$  [15, 16], and IL-6 [15] release in several models of inflammatory pain. Naringenin also inhibits RANKL-induced osteoclastogenesis and bone resorption through suppression of the p38 MAPK phosphorylation inhibiting osteolysis in titanium particles-induced calvarial osteolysis [17].

In general, the inflammatory response includes the development of clinical signs such as increase in local or systemic temperature, erythema, edema, and pain [18]. These clinical symptoms directly affect patients' quality of life [19]. The analgesic, anti-inflammatory, and anti-osteolytic properties of naringenin [14–16, 20] would be important activities in the context of prosthesis-induced inflammation. Considering the physiopathology and clinical symptoms of prosthesis-induced arthritis as well as the pharmacological evidence on the activities of naringenin, we reason that naringenin has pharmacological potential on the treatment of prosthesis-induced arthritis. Thus, in the present study, we evaluated the therapeutic effect and mechanisms of the action

of naringenin in the pathogenesis of TiO<sub>2</sub>-induced chronic arthritis.

## Materials and methods

### General experimental procedures

In the first series of experiments, mice ( $n=6$  per group per experiment) were stimulated in the right joint with an intra-articular (i.a.) injection of 3 mg of TiO<sub>2</sub> per knee joint as described previously [10]. 24 h after TiO<sub>2</sub> stimulus, mice were treated daily with titrated doses of naringenin [16.7, 50, or 150 mg/kg, per oral (p.o.)] [14]. Mechanical hyperalgesia and knee joint volume (e.g., edema) evaluation started 24 h after TiO<sub>2</sub> stimuli and occurred every other day before and after naringenin treatment (1 h, 3 h, 5 h, 7 h, and 24 h after naringenin treatment in the first day and 1 h after naringenin treatment once a day up to 30 days) [10, 21]. The naringenin dose of 50 mg/kg was chosen based on the results of hyperalgesia and edema. Stomach and blood samples were harvested on the 30th day to evaluate the possible side effects and toxic effects of chronic naringenin treatment. Parameters were stomach myeloperoxidase (MPO) activity, and plasmatic levels of aspartate transaminase (AST), alanine transaminase (ALT), urea, and creatinine. Knee joint and knee joint lavages were collected for histopathology [hematoxylin–eosin stain (HE)] and leukocytes recruitment analyses. Cartilage damage was determined with toluidine blue staining and patella proteoglycan levels. Bone resorption was evaluated by histochemical staining tartrate-resistant acid phosphatase (TRAP; a marker of osteoclasts) and RANKL/RANK/OPG signalling pathway by RT-qPCR. Oxidative stress was evaluated with gp91<sup>phox</sup> mRNA expression [RT-qPCR], superoxide anion [nitroblue tetrazolium reduction levels], and lipid peroxidation (thiobarbituric acid reactive substances [TBARS]), and pro-inflammatory cytokines mRNA expression (TNF $\alpha$ , proIL-1 $\beta$ , IL-6 and IL-33), and NF $\kappa$ B activation (ELISA) were analyzed with the mentioned methods. Free movements of animals were not altered by i.a. injection of TiO<sub>2</sub>. The 30 days final time point was selected in preliminary experiments aiming to determine joint cartilage and bone damage [14], which were known not to occur before 7 days of TiO<sub>2</sub> inflammation [21]. All experiments were performed blinded.

### Animals

Male Swiss mice weighing between 20 and 25 g from the Londrina State University, Londrina, Paraná, Brazil, were used in this study. Mice were housed in standard clear plastic cages with water and food ad libitum, light/dark cycle of 12/12 h and controlled temperature (21 °C). Mice were

maintained in the vivarium of the Department of Pathology of Londrina State University for at least 2 days before experiments. Mice were used only once and were acclimatized to the testing room at least 1 h before the experiments, which were conducted during the light cycle. Animal care and handling procedures were in accordance with the International Association for Study of Pain (IASP) guidelines and approved by the Londrina State University Ethics Committee on Animal Research and Welfare (process number 11849.2015.19). All efforts were made to minimize the number of animals used and their suffering.

### Test compounds

The compounds used in this study were saline solution (NaCl 0.9%; Frenesius Kabi Brasil Ltda, Aquiraz, CE, Brazil), ethylenediaminetetraacetic acid disodium salt (EDTA; Synth, Diadema, SP, Brazil), and naringenin (Santa Cruz Biotechnology, Inc., 98%, Dalla, TX, USA). Titanium dioxide was purchased from Synth (Diadema, SP, Brazil), and the particle size was < 1 µm with an average of 862.2 nm as determined by size distribution analysis (Malvern Instruments Ltd, UK). Immediately before the injections, TiO<sub>2</sub> was suspended in sterile saline (10 µL) and naringenin was diluted in sterile saline solution. Naringenin (16.7, 50, or 150 mg/kg) and saline were administered by p.o. in a volume of 100 µL.

### Evaluation of articular mechanical hyperalgesia

The knee joint mechanical hyperalgesia was evaluated as previously described [22]. Briefly, in a quiet room, mice were placed individually in acrylic cages (12 × 10 × 17 cm) with a wire grid floor 15–30 min before the test for environmental adaptation. An electronic pressure-meter test consisting of a handheld force transducer fitted with a polypropylene tip (electronic von Frey Anesthesiometer; Insight, Ribeirão Preto, SP, Brazil) was used to evaluate mechanical articular nociception. For this model, a large tip (4.15 mm<sup>2</sup>) was adapted to the probe. An increasing perpendicular force was applied to the central area of the plantar surface of the hind paw to induce a flexion movement of the tibiofemoral joint followed by paw withdrawal. The electronic pressure-meter apparatus automatically recorded the intensity of the force applied when the paw was withdrawn. The flexion-elicited mechanical threshold was expressed in grams (g) [22].

### Articular edema measurements

Articular edema of the tibiofemoral joint was assessed through measurements of the transverse diameters using a caliper (Digmatic Caliper, Mitutoyo Corporation, Kanagawa, Japan). Thickness values of the femorotibial

joint were expressed as the percentage change by the ratio between the delta (the difference between the diameters measured before [basal value] and after TiO<sub>2</sub> i.a. injection) and basal value multiplied by 100.

### Histopathology

Joints were fixed in 4% formaldehyde for 2 days before decalcification in NaOH/EDTA solution (pH 7.3–7.4) and processed for paraffin embedding. Tissue longitudinal sections (7 µm) were prepared and stained with HE. HE-stained tibiofemoral joint sections were examined blinded and scored by a pathologist using light microscopy, and the degree of synovial hyperplasia, inflammatory infiltrate, and vascular proliferation were determined with modifications as described previously [23, 24]. The degrees of the following parameters were: (a) synovial hyperplasia (from 0 = no pannus formation, to 3 = most severe pannus formation); (b) inflammatory infiltrate (from 0 = no inflammation, to 3 = most severe inflammation); and (c) vascularity (from 0 = no vascular proliferation, to 3 = most severe proliferation). Regarding vascular proliferation, it was considered the quantity of the capillary blood vessels. The final score was determined by summing all three parameters (a–c) resulting in a score for each sample expressed as the mean of six samples accordingly to the groups.

### Myeloperoxidase activity

Myeloperoxidase (MPO) activity was used to evaluate possible naringenin-induced gastric damage, considering its activity increases with gastric damage induced by non-steroidal anti-inflammatory drugs [25]. Samples of the stomach were harvested in 50 mM K<sub>2</sub>HPO<sub>4</sub> buffer (pH 6.0) containing 0.5% hexadecyl trimethylammonium bromide (HTAB) and kept at –86 °C until use. Frozen samples were homogenized using a tissue turrax (Tissue-Tearor 985370, BioSpec Products, Bartlesville, OK, USA) and centrifuged (2 min, 16,000g, 4 °C), and the resulting supernatant was assayed using a spectrophotometer (Multiskan GO Microplate Spectrophotometer, ThermoScientific, Vantaa, Finland) for MPO activity determination at 450 nm. The MPO activity of samples was compared to a standard curve of neutrophils. Briefly, 15 µL of sample was mixed with 200 µL of 50 mM phosphate buffer (pH 6.0), containing 0.167 mg/mL *O*-dianisidine dihydrochloride and 0.0005% hydrogen peroxide. Indomethacin (2.5 mg/kg, i.p., diluted in tris/HCl buffer, for 7 days) was used as positive drug control for stomach damage. The results were presented as MPO activity (number of neutrophils × 10<sup>6</sup>/mg of tissue).

## Liver and kidney toxicity assays

Blood was harvested into microtubes containing 50  $\mu\text{L}$  of the anticoagulant EDTA (5000 IU/mL) and centrifuged (200g, 10 min, 4 °C), and the plasma was separated. To determine naringenin-induced liver and kidney toxicity, plasma samples were used. Aspartate aminotransferase (AST) and alanine aminotransferase (ALT) were used as markers of hepatotoxicity, and acetaminophen was used as a positive drug control (650 mg/kg, intraperitoneal [i.p.], diluted in sterile saline, once). Urea and creatinine levels were used to evaluate nephrotoxicity, and diclofenac was a positive drug control (200 mg/kg, orally, diluted in sterile saline, once). Plasma samples were processed according to the manufacturer's instructions (Labtest Diagnóstico S. A., Brazil). Results were presented as U/mL (AST and ALT) or mg/dL (urea and creatinine) of plasma.

## Evaluation of leukocyte migration

The total and differential counts of recruited leukocytes to the knee joint cavity were determined as previously described [26]. Briefly, knee joint cavities were washed with saline containing EDTA, which was recovered to evaluate total and differential cell counts. Total cell counts were performed in Neubauer chamber using Turk solution, and differential cell counts (100 cells per slide) were performed in slices stained with the panoptic kit (Laborclin, Pinhais, PR, Brazil) under a light microscope (Olympus CX31RTSF, Tokyo, Japan). Results were expressed as total leukocytes, polymorphonuclear, and mononuclear cells (cells  $\times 10^3$ /knee joint).

## Proteoglycan assays

Proteoglycan degradation was evaluated using toluidine blue staining in samples processed for histopathology [21]. The percentage of stained areas (femoral and tibial cartilages) was measured using ImageJ 1.50i software. The load-bearing region was outlined in black and the same minimum (170) and maximum (255) threshold values for each sample analysis were used. Proteoglycan concentration was determined in patella using a colorimetric assay [27]. Briefly, the patella was carefully collected from mice and fixed with formaldehyde (4%) overnight using a shaker and decalcified in formic acid (5%) for 4 h using a shaker. Each patella sample was digested at 60 °C for 16 h with 60  $\mu\text{L}$  of papain digestion buffer (5 mg/mL) in calcium- and magnesium-free PBS with 5 mM cysteine and 10 mM EDTA, pH 7.4. After reaching room temperature, samples were centrifuged for 10 min at 1000g to collect the condensation droplets. Next, 50  $\mu\text{L}$  of the supernatants and of serial chondroitin sulfate solutions (standard curve; 50–1000 mg/mL) was placed into

96-well plates. Then, 300  $\mu\text{L}$  of a 1,9-dimethylmethylene blue (DMMB; 50 mg/L, Polysciences) solution was added to each well, and proteoglycan contents [21] were determined by spectrophotometer reading at 525 nm (Multiskan GO Microplate Spectrophotometer, ThermoScientific, Vantaa, Finland). The glucosaminoglycan (GAG) knee joint content was calculated from a standard curve using chondroitin 6-sulfate sodium salt from shark cartilage as standard. Results were presented as proteoglycan per milligram (mg) of tissue.

## Histochemical stain for TRAP

TRAP was used as a histochemical marker of osteoclasts activation in 6  $\mu\text{m}$  sections [10]. Sections were stained according to TRAP kit 387A (Sigma–Aldrich, St. Louis, MO, USA) and TRAP-positive cells appeared as dark purple. Digitally acquired images were analyzed in the ImageJ 1.44 software, using the threshold tool with color-based selection for positive staining analyzed in a total area of 3,145,728 pixels, which is a maximum area that can be acquired with our equipment (Olympus CX31RTSF, Tokyo, Japan coupled with lumenera Infinity 1 microscope camera, Ottawa, Canada). Three slices per sample of knee joint tissue were analyzed and data were averaged. Results were expressed by total stained pixels of TRAP staining. Control and experimental knee joints were processed under the same conditions.

## Nitroblue tetrazolium reduction

The superoxide anion production was determined by the reduction of the redox dye nitroblue tetrazolium (NBT) [28]. Knee joint frozen tissue from mice were homogenized with 500  $\mu\text{L}$  of saline using an ultra-turrax (Tissue-Tearor 985370, BioSpec Products, Bartlesville, OK, USA) and centrifuged (10 min, 3,300 g, 4 °C), and 50  $\mu\text{L}$  of the homogenate was placed in a 96-well plate, followed by the addition of 100  $\mu\text{L}$  of nitroblue tetrazolium solution (1 mg/mL) (NBT, Sigma) and maintained at 37 °C in a warm bath for 5 min. The supernatant was removed, and the formazan precipitated was then solubilized by adding 120  $\mu\text{L}$  of 2 M KOH and 120  $\mu\text{L}$  of dimethylsulfoxide (DMSO). The optical density was measured using a microplate spectrophotometer reader (Multiskan GO Microplate Spectrophotometer, ThermoScientific, Vantaa, Finland) at 600 nm. The NBT reduction levels were corrected per the total protein concentration and the results were presented as NBT reduction (OD/mg of protein).

## Lipid peroxidation

Tissue lipid peroxidation was assessed by the levels of thiobarbituric acid reactive substances (TBARS) [29]. For this

assay, TCA 10% was added to the homogenate and the mixture was centrifuged (3 min, 1000g, 4 °C) to precipitate the proteins. The protein-free supernatant was then separated and mixed with TBA (0.67%). The mixture was kept in a water bath (15 min, 100 °C). Malondialdehyde (MDA), an intermediate product of lipid peroxidation, was determined by the difference between absorbance at 535 and 572 nm using a microplate spectrophotometer reader. The TBARS were corrected per the total protein concentration and the results presented as TBARS ( $\Delta OD A_{535} - A_{572}$  /mg of protein) [29].

## RT-qPCR

The knee joint was dissected 30 days after TiO<sub>2</sub> and homogenized in TRIzol reagent<sup>®</sup>. Total RNA was extracted by using the SV Total RNA Isolation System (Promega). The purity of total RNA was measured using a spectrophotometer (Multiskan GO Microplate Spectrophotometer, Thermo Scientific, Vantaa, Finland) and the wavelength absorption ratio (260/280) was between 1.8 and 2.0 for all preparations. Reverse transcription of total RNA to cDNA and qPCR was carried out using GoTaq<sup>®</sup> 2-Step RT-qPCR System (Promega) and specific primers. A no-reverse transcription control was applied for cDNA production (running the samples without adding reverse transcriptase enzyme) and a no-template control (NTC) was carried out for qPCR (running the qPCR reaction without cDNA). The qPCR reaction was performed in a StepOnePlus<sup>™</sup> Real-Time PCR System (Applied Biosystems<sup>®</sup>). The relative gene expression was measured using the comparative 2<sup>-( $\Delta\Delta C_q$ )</sup> method. The primers used were: RANKL, sense: 5'-CAG AAG ATG GCA CTC ACT GCA-3', antisense: 5'-CAC CAT CGC TTT CTC TGC TCT-3'; RANK, sense: 5'-CTA ATC CAG CAG GGA AGC AAAT-3', antisense: 5'-GAC ACG GGC ATA GAG TCA GTTC-3'; osteoprotegerin (OPG), sense: 5'-GGA ACC CCA GAG CGA AAT ACA-3', antisense: 5'-CCT GAA GAA TGC CTC CTC ACA-3'; gp91<sup>phox</sup>, sense: 5'-AGC TAT GAG GTG GTG ATG TTA GTGG-3', antisense: 5'-CAC AAT ATT TGT ACC AGA CAG ACT TGAG-3'; TNF $\alpha$ , sense: 5'-TCT CAT CAG TTC TAT GGC CC-3', antisense: 5'-GGG AGT AGA CAA GGT ACAAC-3'; pro-IL-1 $\beta$ , sense: 5'-GAA ATG CCA CCT TTT GAC AGTG-3', antisense: 5'-TGG ATG CTC TCA TCA GGA CAG-3'; IL-6, sense: 5'-GAG GAT ACC ACT CCC AAC AGA CC-3', antisense: 5'-AAG TGC ATC ATC GTT GTT CAT ACA-3'; IL-33, sense: 5'-TCC TTG CTT GGC AGT ATCCA-3', antisense: 5'-TGC TCA ATG TGT CAA CAG ACG-3'; glyceraldehyde 3-phosphate dehydrogenase (Gapdh), sense: 5'-CAT ACC AGG AAA TGA GCT TG-3', antisense: 5'-ATG ACA TCA AGA AGG TGG TG-3';  $\beta$ -actin: sense: 5'-AGC TGC GTT TTA CAC CCT TT-3', antisense: 5'-AAG CCA TGC CAA TGT TGT CT-3'. The

expressions of Gapdh and  $\beta$ -actin mRNA were used as the reference gene, and the results were expressed as mRNA expression (normalized to Gapdh and  $\beta$ -actin).

## NF $\kappa$ B activation

The knee joint samples were homogenized in 400  $\mu$ L of the appropriate buffer containing protease inhibitors. The homogenates were centrifuged (10 min, 16,100g, 4 °C), and the supernatants were used to assess the levels of phosphorylated and total NF $\kappa$ B p65 subunit by ELISA using PathScan<sup>®</sup> kits (Cell Signaling) at 450 nm (Multiskan GO Thermo Scientific) according to the manufacturer's directions. The phosphorylated and total NF $\kappa$ B p65 subunit were corrected per the total protein concentration and the results are expressed as NF $\kappa$ B activation (IoD phospho-p65/totalp65 ratio/mg of protein).

## Statistical analysis

The results are presented as means  $\pm$  SEM of measurements made on six mice in each group per experiment and are representative of two separate experiments. Two-way repeated measures analysis of variance (ANOVA) followed by Tukey's post hoc was used to compare all groups and doses at all times when responses were measured at different times after the stimulus injection. Differences between responses were evaluated by one-way ANOVA followed by Tukey's post hoc for data of single time point. Statistical differences were considered significant when  $p < 0.05$ .

## Results

### Naringenin inhibits TiO<sub>2</sub>-induced mechanical hyperalgesia and edema without inducing toxicity

Mice were treated with naringenin (16.7, 50, or 150 mg/kg) by p.o. route starting 24 h after the i.a. injection of 3 mg/joint of TiO<sub>2</sub>. Animals were treated daily for 30 days, 1 h before the articular mechanical hyperalgesia and edema measurements since naringenin peak-effect in mechanical hyperalgesia at day 1 occurred 1 h after naringenin treatment (Fig. 1a). The saline group did not present articular mechanical hyperalgesia (Fig. 1a) and edema (Fig. 1b). The i.a. injection of TiO<sub>2</sub> at day 0 induced articular mechanical hyperalgesia (Fig. 1a) and edema (Fig. 1b) from 24 to 48 h after i.a. injection on the first day and subsequently from the 2nd to 30th day. All doses of naringenin inhibited TiO<sub>2</sub>-induced articular mechanical hyperalgesia at day 1. Naringenin effect lasted less than 24 h, thus daily treatment was required. Naringenin treatment inhibited TiO<sub>2</sub>-induced articular mechanical hyperalgesia from the 2nd to 30th day.

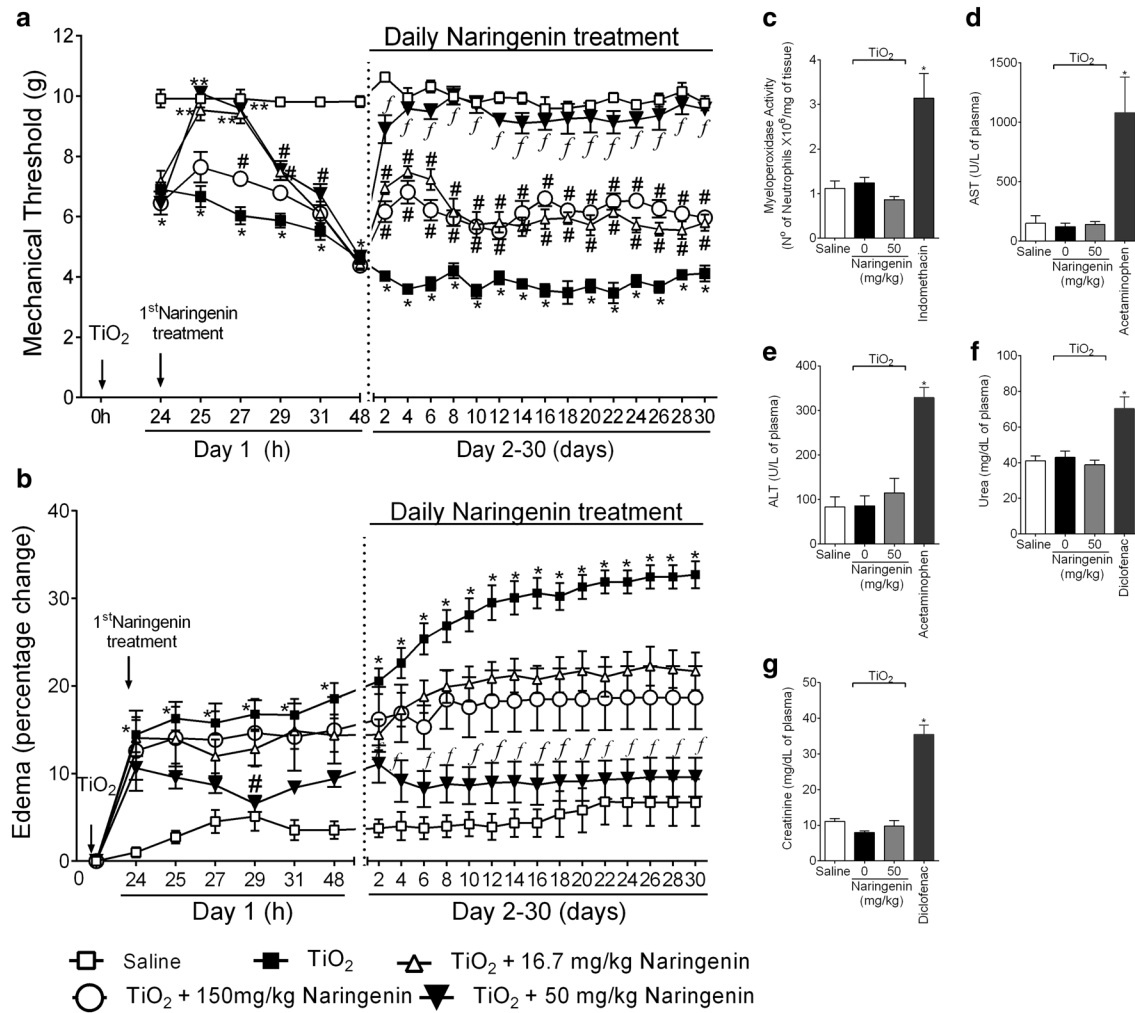


**Fig. 1** Naringenin inhibits TiO<sub>2</sub>-induced articular mechanical hyperalgesia and edema without inducing toxicity. Mice were treated daily for 30 days with naringenin (16.7, 50, or 150 mg/kg, p.o.) starting 24 h after intra-articular injection of TiO<sub>2</sub> (3 mg/joint). **a** Articular mechanical hyperalgesia and **b** edema were measured initially from 24 to 48 h (day 1) after TiO<sub>2</sub> injection and subsequently every other day until day 30 after TiO<sub>2</sub> injection (days 2–30). At day 30, naringenin induced **c** MPO activity in the stomach, **d** AST, and **e** ALT plasmatic levels; **f** urea, and **g** creatinine plasmatic levels were determined to evaluate treatment toxicity. As positive drug control for gastric, hepatic, and renal toxicity, indomethacin (2.5 mg/kg, i.p., diluted

in tris/HCl buffer, during 7 days), acetaminophen (650 mg/kg, i.p., diluted in saline), and diclofenac (200 mg/kg, p.o., diluted in saline, once) were used, respectively. Results are presented as mean  $\pm$  SEM of six mice per group per experiment and are representative of two separate experiments. [ $*p < 0.05$  compared to the saline group;  $\#p < 0.05$  compared to the TiO<sub>2</sub> group;  $**p < 0.05$  compared to the TiO<sub>2</sub> and naringenin (150 mg/kg) groups;  $fp < 0.05$  compared to the TiO<sub>2</sub> and naringenin (16.7 and 150 mg/kg) groups (repeated measures two-way ANOVA (**a**, **b**) and one-way ANOVA (**c**–**g**) followed by Tukey's post hoc]

The dose of 16.7 mg/kg inhibited TiO<sub>2</sub>-induced articular mechanical hyperalgesia from 1 to 5 h after the treatment (25–29 h after TiO<sub>2</sub> i.a. injection) on day 1 and up to 30 days. The dose of 50 mg/kg of naringenin inhibited TiO<sub>2</sub>-induced articular mechanical hyperalgesia from 1 to 7 h after the treatment (25–31 h after TiO<sub>2</sub> i.a. injection) on day 1 and subsequently from days 2 to 30. In addition, the analgesic effect of the dose of 50 mg/kg of naringenin was statistically different compared to the other doses from days 2 to 30. The dose of 150 mg/kg of naringenin inhibited TiO<sub>2</sub>-induced articular mechanical hyperalgesia only 5 h after naringenin

treatment (29 h after TiO<sub>2</sub> i.a. injection) at day 1 and up to 30 days (Fig. 1a). Only the dose of 50 mg/kg of naringenin inhibited TiO<sub>2</sub>-induced articular edema 5 h after naringenin treatment (29 h after TiO<sub>2</sub> i.a. injection) at day 1 and from days 4 to 30. In addition, the inhibition of edema by a dose of 50 mg/kg of naringenin was statistically different compared to the other doses (Fig. 1b). Therefore, naringenin presented a bell-shaped dose–response curve with maximal effect with the dose of 50 mg/kg, which was chosen for the next experiments. At day 30, 1 h after naringenin treatment, stomach and blood samples were collected to evaluate if naringenin

would induce gastric, hepatic, and renal damage. Naringenin did not induce MPO activity in stomach samples (Fig. 1c) or increase the levels of AST (Fig. 1d), ALT (Fig. 1e), urea (Fig. 1f), and creatinine (Fig. 1g) in the plasma. Therefore, chronic 30 days treatment with naringenin at a dose of 50 mg/kg did not induce detectable gastric, hepatic, or renal lesion/damage. The treatment with positive control groups following previously established protocols demonstrates that the assays used can detect the selective tissue lesion markers [10, 28] (Fig. 1c–g).

### **Naringenin inhibits TiO<sub>2</sub>-induced histopathological damage, recruitment of total leukocytes, polymorphonuclear, and mononuclear cells**

Mice were treated daily for 30 days with naringenin (50 mg/kg, p.o.) starting 24 h after the i.a. injection of 3 mg/joint of TiO<sub>2</sub>. At day 30, 1 h after naringenin treatment, the knee joint was harvested for HE histopathology (Fig. 2a–g) evaluation and knee joint lavages were collected to count the number of total leukocytes (Fig. 2h), polymorphonuclear (Fig. 2i), and mononuclear cells (Fig. 2j). Naringenin inhibited TiO<sub>2</sub>-induced synovial hyperplasia, inflammatory infiltrate, and vascular proliferation as observed in the histopathological index analyses (Fig. 2g). In agreement, naringenin inhibited TiO<sub>2</sub>-induced recruitment of total leukocytes (Fig. 2h) and polymorphonuclear (Fig. 2i) and mononuclear cells (Fig. 2j) to the knee joint. Thus, naringenin reduced the recruitment of inflammatory cells induced by TiO<sub>2</sub> in the knee joint.

### **Naringenin inhibits TiO<sub>2</sub>-induced cartilage erosion in the knee joint**

Mice were treated as in Fig. 2 and knee joint samples were collected for toluidine blue staining of cartilage and analyses (Fig. 3a–k). Patella samples were also collected for the determination of proteoglycan levels (Fig. 3i). TiO<sub>2</sub> decreased toluidine blue-stained cartilage area (Fig. 3b, e, h) in the tibia (Fig. 3b, h, k), but not in the femur (Fig. 3b, e, j) and patella proteoglycan content (Fig. 3i). Naringenin inhibited TiO<sub>2</sub>-decreased toluidine blue staining cartilage in the tibia (Fig. 3c, i, k) and patella proteoglycan content (Fig. 3l). These results demonstrate that naringenin inhibited TiO<sub>2</sub>-induced cartilage destruction.

### **Naringenin inhibits TiO<sub>2</sub>-induced bone resorption**

Mice were treated as in Fig. 2 and knee joint samples were collected to evaluate the TRAP staining (osteoclast marker) and the mRNA expression by RT-qPCR of the RANKL/RANK/OPG system. TiO<sub>2</sub> induced an increase of TRAP staining (Fig. 4b, e, g) and the RANKL mRNA expression (Fig. 4h),

which were inhibited by naringenin treatment. TiO<sub>2</sub> did not alter the mRNA expression of RANK (Fig. 4i) and decreased OPG expression (Fig. 4j), but naringenin reduced the RANK mRNA expression and increased OPG mRNA expression. Therefore, naringenin inhibited TiO<sub>2</sub>-induced dysregulation of markers of increased bone resorption [10, 30, 31].

### **Naringenin inhibits TiO<sub>2</sub>-induced oxidative stress**

Animals were treated as in Fig. 2 and knee joint samples were collected to evaluate the effect of naringenin on TiO<sub>2</sub>-induced oxidative stress. TiO<sub>2</sub> induced an increase of gp91<sup>phox</sup> mRNA expression (Fig. 5a), and the production of superoxide anion (Fig. 5b) and lipid peroxidation (Fig. 5c), which were inhibited by naringenin treatment. Thus, this demonstrated that naringenin not only inhibited TiO<sub>2</sub>-induced oxidative stress, but also the upregulation of a NADPH oxidase (NOX)2 subunit involved in superoxide anion production [32].

### **Naringenin inhibits TiO<sub>2</sub>-induced cytokines mRNA expression**

Mice were treated as in Fig. 2 and the knee joint samples were collected to evaluate IL-33, TNF $\alpha$ , pro-IL-1 $\beta$ , and IL-6 mRNA expression. TiO<sub>2</sub> induced the expression of TNF- $\alpha$  (Fig. 6a), pro-IL-1 $\beta$  (Fig. 6b), IL-6 (Fig. 6c), and IL-33 (Fig. 6d) mRNA expression, which were inhibited by naringenin treatment. Therefore, naringenin reduced the TiO<sub>2</sub>-induced expression of pro-inflammatory cytokines involved in pain, edema, leukocyte recruitment, and joint tissue degradation [26, 30, 33–41].

### **Naringenin inhibits TiO<sub>2</sub>-induced NF $\kappa$ B activation**

Considering that naringenin inhibited TiO<sub>2</sub>-induced oxidative stress and the mRNA expression of enzymes and cytokines that are regulated by NF $\kappa$ B activation [42, 43], mice were treated as in Fig. 2 and knee joint samples were collected to evaluate NF $\kappa$ B activation by ELISA (Fig. 7). TiO<sub>2</sub> induced an increase in phosphorylated p65 NF $\kappa$ B/total p65 NF $\kappa$ B ratio, indicating NF $\kappa$ B activation (phosphorylation), which was inhibited by naringenin treatment (Fig. 7). Therefore, naringenin inhibited the TiO<sub>2</sub>-induced activation of a crucial pro-inflammatory transcription factor, NF $\kappa$ B. The present results are summarized in Fig. 8.

## **Discussion**

Arthroplasty is an efficient and successful procedure to recover joint mobility and functionality [4]. However, about 10–15% of the patients present intense inflammatory

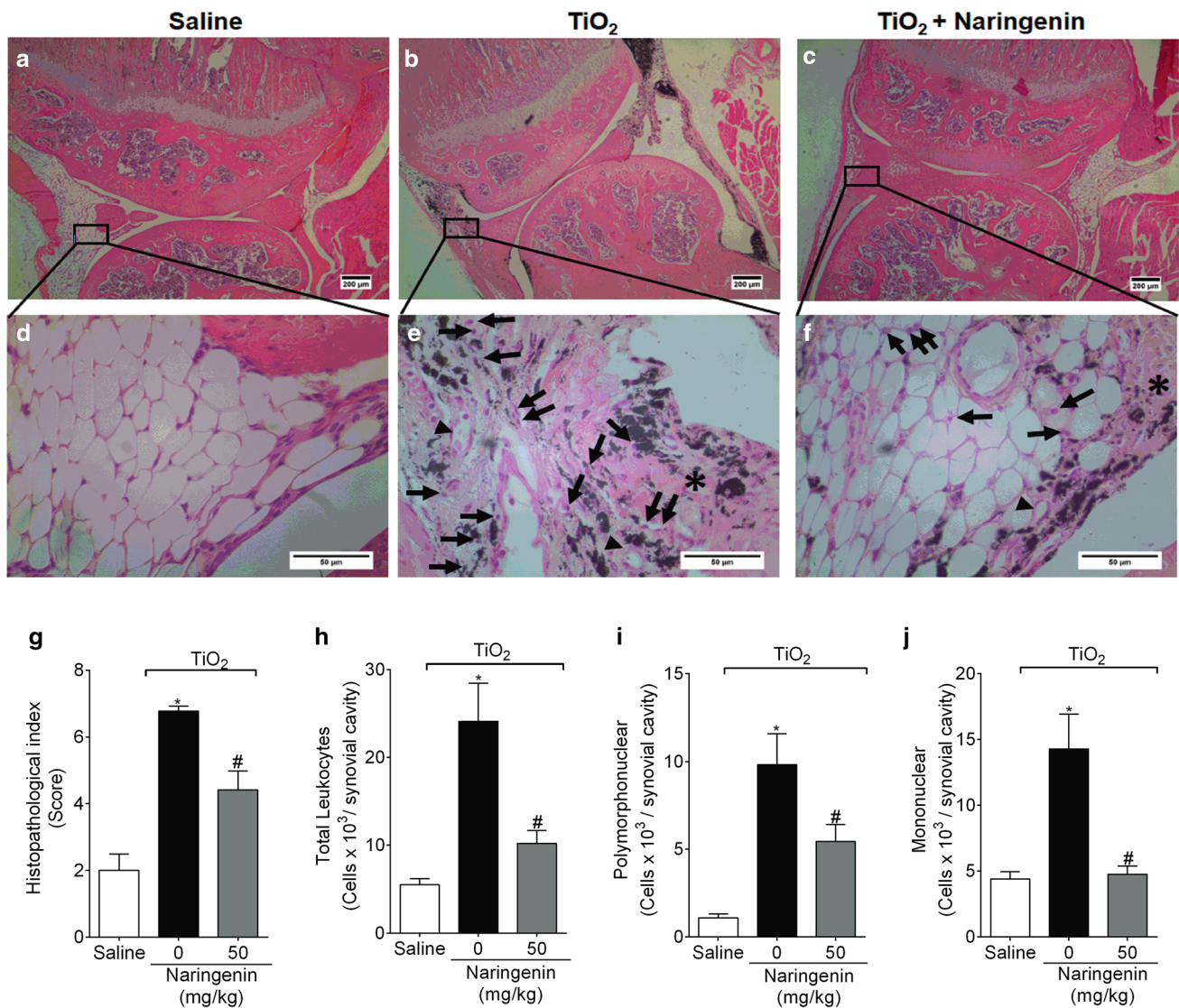


**Fig. 2** Naringenin inhibits TiO<sub>2</sub>-induced histopathological damage, recruitment of total leukocytes and polymorphonuclear and mononuclear cells. Mice were treated daily for 30 days with naringenin (50 mg/kg, p.o.) starting 24 h after intra-articular injection of TiO<sub>2</sub> (3 mg/joint). Histopathological analysis (a–f) and index (g), total leukocytes (h), and polymorphonuclear (i) and mononuclear cell (j) count in knee joint lavages were evaluated 30 days after TiO<sub>2</sub> injection. The sites where the images of d–f were captured were from a to c. The parameters analyzed were (asterisk) invasive pannus forma-

tion; leukocyte infiltration was represented by an arrow; and vascularity with an arrowhead. Saline (a and d); TiO<sub>2</sub> (b and e); and TiO<sub>2</sub> treated with naringenin (c and f). The samples were stained with HE. Original magnification 4× (scale bar 200 μm) and 40× (scale bar 50 μm), n=6. Results are presented as mean ± SEM of six mice per group per experiment and are representative of two separate experiments. [\*p < 0.05 compared to the saline group; #p < 0.05 compared to the TiO<sub>2</sub> group (one-way ANOVA followed by Tukey's post hoc)]

response triggered by wear debris released by biomaterials [6, 44]. TiO<sub>2</sub> is one of the main biomaterials used in the metallic prosthesis and implants and also a causative agent of articular inflammation and loosening of prosthesis and implants [9, 45]. In the present study, data show that naringenin reduced TiO<sub>2</sub>-induced arthritic pain, edema, and leukocyte recruitment to the knee joint. These beneficial effects of naringenin were related to the reduction of oxidative stress and cytokine expression, which are consequences

of naringenin inhibition of TiO<sub>2</sub>-induced NFκB activation. Naringenin effect occurred in a bell-shaped dose–response curve indicating that naringenin treatment reached a maximum effect at a dose and increasing naringenin dose does not improve but rather reduces its efficacy. If naringenin goes through clinical testing, a dose range for naringenin must be determined and increasing the dose indefinitely will not necessarily increase its efficacy. Considering that naringenin acts as an antioxidant, and other flavonoids such as myricetin



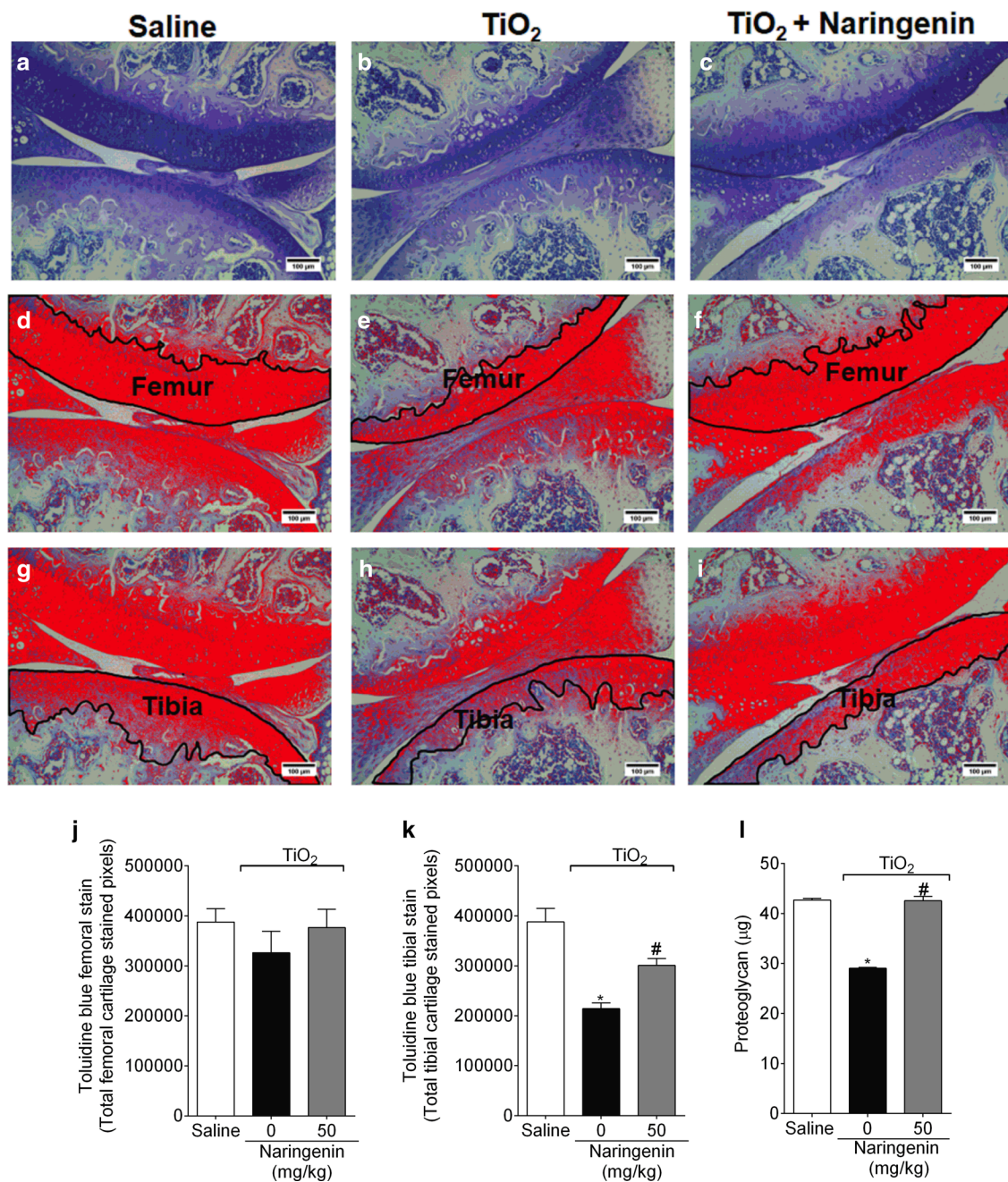


**Fig. 3** Naringenin inhibits TiO<sub>2</sub>-induced cartilage erosion in the knee joint. Mice were treated daily for 30 days with naringenin (50 mg/kg, p.o.) starting 24 h after intra-articular injection of TiO<sub>2</sub> (3 mg/joint). **a–i** Toluidine blue staining quantification of **j** femoral and **k** tibial-stained areas; and **l** quantitative quantification of proteoglycan levels in the knee joint samples were evaluated on the 30th day. **a, d, g** Saline; **b, e, h** TiO<sub>2</sub>; and **c, f, i** TiO<sub>2</sub> treated with naringenin. The percentage of toluidine blue-stained areas in the **j** femoral and **k** tibial

cartilage in the load-bearing region were measured through the area outlined in black. **d–f** and **g–i** demonstrate the analysis performed in the femur and tibia, respectively. Original magnification 10× (scale bar 100 μm), *n* = 6. Results are presented as mean ± SEM of six mice per group per experiment and are representative of two separate experiments. [\**p* < 0.05 compared to the saline group; #*p* < 0.05 compared to the TiO<sub>2</sub> (one-way ANOVA followed by Tukey's post hoc)]

inverse their antioxidant effects to pro-oxidant effect at high doses, it is reasonable to speculate that upon reaching the maximal antioxidant dose, higher doses of naringenin may start reducing the intended effect similarly to myricetin [46].

Evidence shows that the analgesic mechanisms of naringenin may encompass the targeting of nociceptive neurons function. For instance, naringenin modulates transient potential receptors (TRP) by blocking TRPV1 and TRPM3 and

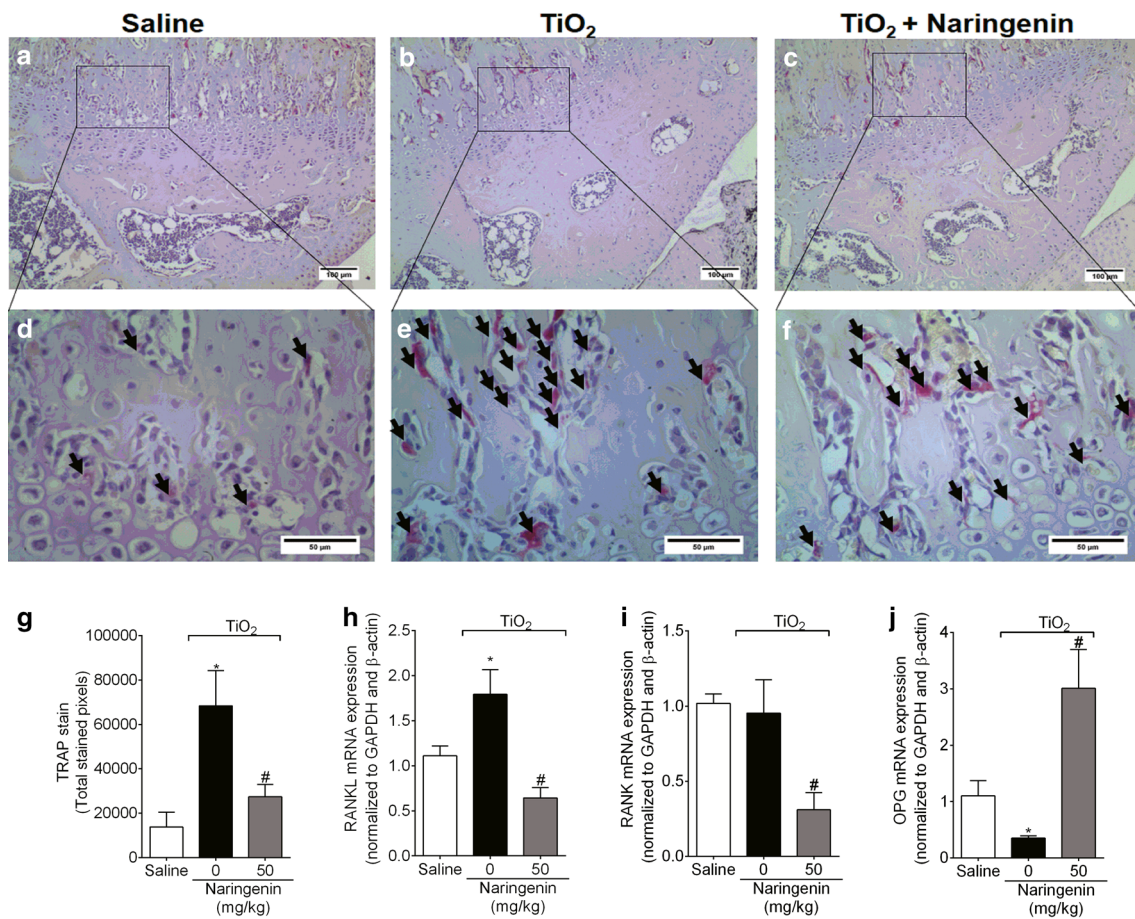


**Fig. 4** Naringenin inhibits TiO<sub>2</sub>-induced bone resorption. Mice were treated daily for 30 days with naringenin (50 mg/kg, p.o.) starting 24 h after TiO<sub>2</sub> i.a. injection (3 mg/joint). **a–f** TRAP histochemical staining; **g** quantitative analysis of TRAP-positive cells; **g** RANKL, **i** RANK, and **j** OPG mRNA expression were determined on the 30th day. The areas delimited in rectangles in **a–c** represent the fields observed in **d–f** that were used to determine **g** TRAP histochemical

staining between the groups. Original magnification 10× (scale bar 100 μm) and 40× (scale bar 50 μm), *n* = 6. Results are presented as mean ± SEM of six mice per group for histochemical stain and qPCR analysis per experiment and are representative of two separate experiments. [\**p* < 0.05 compared to the saline group; #*p* < 0.05 compared to the TiO<sub>2</sub> group (one-way ANOVA followed by Tukey's test)]

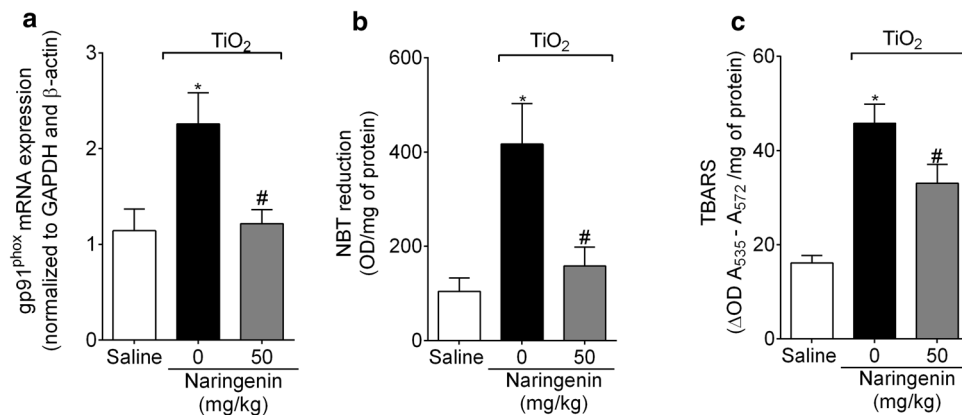


**Fig. 5** Naringenin inhibits TiO<sub>2</sub>-induced oxidative stress. Mice were treated daily for 30 days with naringenin (50 mg/kg, p.o.) starting 24 h after TiO<sub>2</sub> i.a. injection (3 mg/joint). **a** gp91<sup>phox</sup> mRNA expression, **b** superoxide anion production, and **c** TBARS levels were determined on the 30th day after TiO<sub>2</sub> injection. Results are presented as

mean ± SEM of six mice per group per experiment and are representative of two separate experiments. [\**p* < 0.05 compared to the saline group; #*p* < 0.05 compared to the TiO<sub>2</sub> group (one-way ANOVA followed by Tukey's post hoc)]

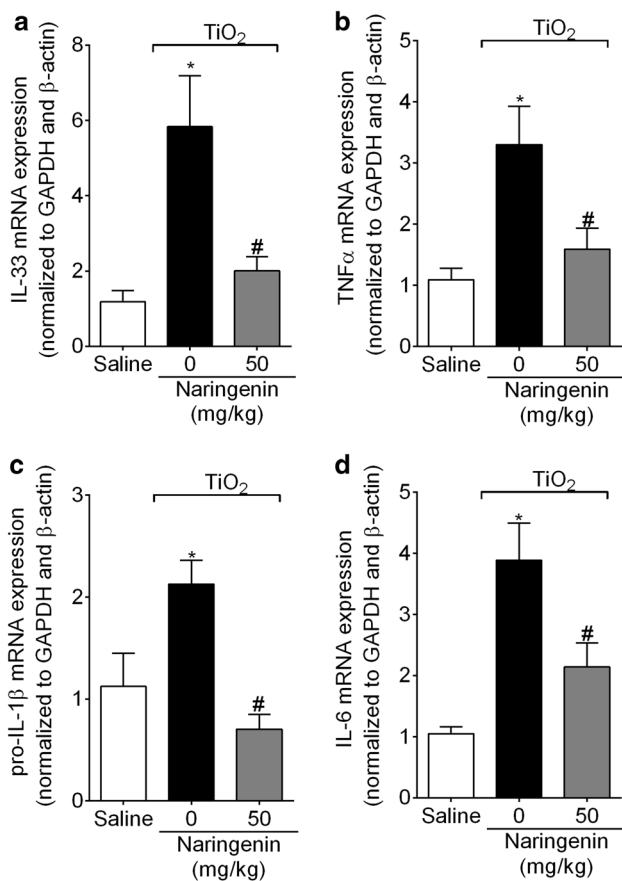


**Fig. 6** Naringenin inhibits TiO<sub>2</sub>-induced cytokines mRNA expression. Mice were treated daily for 30 days with naringenin (50 mg/kg, p.o.) starting 24 h after TiO<sub>2</sub> i.a. injection (3 mg/joint). **a** IL-33, **b** TNF $\alpha$ , **c** pro-IL-1 $\beta$ , and **d** IL-6, mRNA expression were determined by RT-qPCR 30 days after TiO<sub>2</sub> injection. Results are presented as mean  $\pm$  SEM of six mice per group per experiment and are representative of two separate experiments. [\**p* < 0.05 compared to the saline group; #*p* < 0.05 compared to the TiO<sub>2</sub> group (one-way ANOVA followed by Tukey's post hoc)]

activating TRPM8 [47, 48]. Naringenin also activates the analgesic NO-cGMP-PKG-K<sub>ATP</sub> channel signaling pathway [14, 16]. These data indicate that the analgesic effect of naringenin can also target the nociceptive neurons and not solely the peripheral inflammation as we demonstrated herein. In this sense, these results add to each other since they present different perspectives. Naringenin presented a pronounced effect on TiO<sub>2</sub>-induced knee edema, which lined up well with the inhibition of oxidative stress and cytokines since these molecules induce edema [49–51]. Depending on the underlying physiopathological mechanisms of the arthritis type and its degree of severity, therapeutic approaches may include the use of opioids, glucocorticoids, non-steroidal anti-inflammatory drugs, and disease-modifying anti-rheumatic drugs [52]. Depending on the drug, doses, and chronicity of use, there are possible side effects including

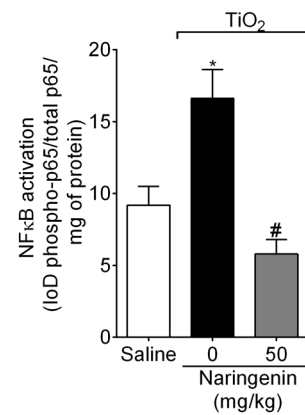


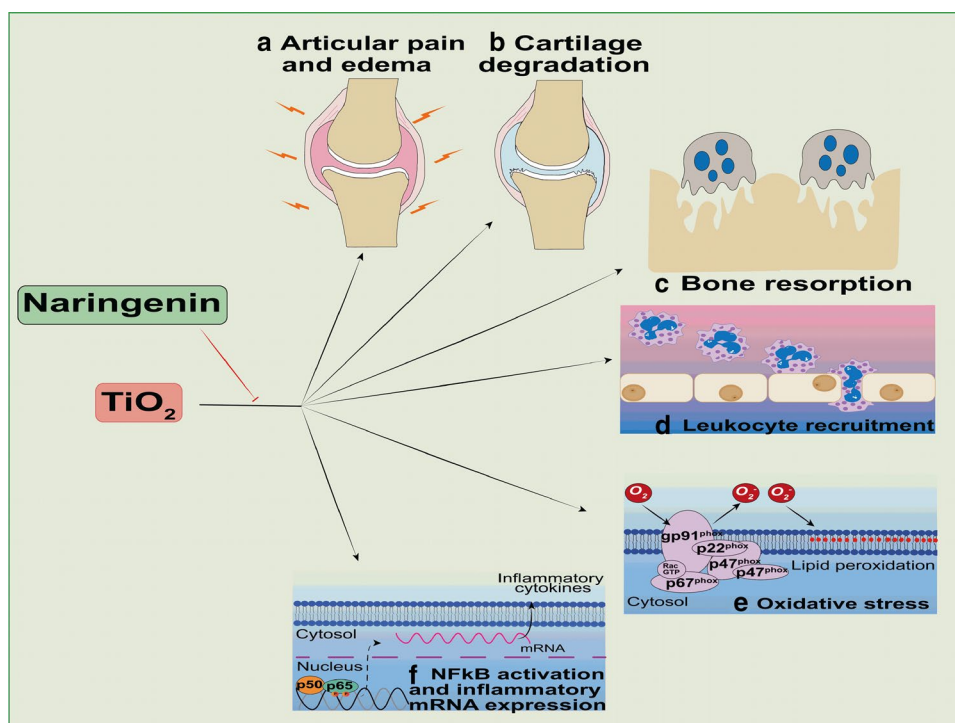
**Fig. 7** Naringenin inhibits TiO<sub>2</sub>-induced NF $\kappa$ B activation. Mice were treated daily for 30 days with naringenin (50 mg/kg, p.o.) starting 24 h after TiO<sub>2</sub> i.a. injection (3 mg/joint). NF $\kappa$ B activation determined 30 days after TiO<sub>2</sub> injection. Results are presented as mean  $\pm$  SEM of six mice per group per experiment and are representative of two separate experiments. [\**p* < 0.05 compared to the saline group; #*p* < 0.05 compared to the TiO<sub>2</sub> group (one-way ANOVA followed by Tukey's post hoc)]

respiratory failure, addiction, gastrointestinal complications, hepatotoxicity, nephrotoxicity, cardiovascular effects, and nausea [53]. The present evidence shows that naringenin is a safe drug given that long-term treatment (30 days) did not induce gastric, hepatic, or kidney damage. Corroborating the safety of naringenin, in vitro cell viability assay demonstrated that naringenin presents low toxicity when compared to other flavonoids, even at a high concentration such as 200  $\mu$ M [54]. Short-term treatment (7 days) with naringenin also does not induce liver and stomach damage [16].

Herein, naringenin inhibited TiO<sub>2</sub>-induced histopathological alterations including severe histopathological damage with vascular proliferation, increased leukocyte infiltration, and pannus formation (synovial hyperplasia) [10]. In agreement, naringenin reduces the histopathological alterations in monoiodoacetate (MIA)-induced osteoarthritis [55]. In addition, naringenin inhibited TiO<sub>2</sub>-induced cartilage destruction and proteoglycan loss. We have previously observed that TiO<sub>2</sub>-induced cartilage destruction with a decrease of proteoglycan content in the knee joint affects mainly the tibia [10]. In agreement with the present data, naringenin inhibits MIA- and IL-1 $\beta$ -induced metalloproteinases (MMP)-3 production in rats cartilage and primary cultured articular chondrocytes, respectively [55]. MMP play important role in cartilage destruction [56] and MMP-3 is well known for proteoglycan degradation and activation of procollagenases [57] This is a very important clinical benefit of naringenin, since once the articular cartilage is destroyed, there is no current treatment to heal it back to pre-disease condition [58].

The pronounced articular inflammation and cartilage destruction fuel the bone loss, which predisposes to bone

**Fig. 8** Naringenin ameliorates  $\text{TiO}_2$ -induced chronic arthritis inhibiting **a** articular pain and edema, **b** cartilage degradation, **c** bone resorption, **d** leukocyte recruitment, **e** oxidative stress, and **f** NF $\kappa$ B activation and mRNA expression of inflammation biomarkers



fractures and increases the severity of motor incapacity and pain.  $\text{TiO}_2$  induced an increase of TRAP staining, which indicates the increase of osteoclastic activity in the bone. The TRAP staining aligned with the increase of RANKL and decrease of OPG mRNA expression, since RANKL induces osteoclast formation and bone resorption and OPG inhibits the activity of RANKL [59, 60]. RANK expression was not altered indicating that the receptor for RANKL already has sufficient expression for enhanced RANKL activity. Naringenin inhibited these alterations in bone metabolism induced by  $\text{TiO}_2$ , and also decreased RANK and increased OPG mRNA expression, which further supports the capacity of naringenin to reduce bone erosion. The cartilage loss facilitates the interaction of recruited neutrophils and osteoclasts. This neutrophil–osteoclast interaction induces osteoclast differentiation [61]. Thus, the cartilage loss and activated inflammatory cells account for increase in bone loss.

Naringenin possesses in vitro and in vivo antioxidant activity [14–16, 54]. In fact, in vitro data show that naringenin presents scavenger ability at 40  $\mu\text{M}$  and molecular docking demonstrated that naringenin reduces NADPH oxidase activation by inhibiting PKC-mediated p47<sup>phox</sup> phosphorylation by interacting with Gly-253 and Leu-251 amino acid residues [54]. In addition, in vivo data show that naringenin also increases Nrf2 activation, a transcription factor that is related to the expression of antioxidant molecules such as GSH [14, 16] suggesting that naringenin not only reduces ROS, but also increases antioxidant defense. In agreement, naringenin inhibits oxidative stress in superoxide

anion- [14] and carrageenan-induced [16] inflammatory pain and streptozotocin-induced diabetic neuropathy [62]. On the other hand, these effects of naringenin seem to impair the microbicidal activity of neutrophils. For instance, naringenin inhibits the killing of *Staphylococcus aureus* by neutrophils [63]. Therefore, given the relationship between oxidative stress and pain, the inhibition of the parameters herein evaluated is an important mechanism of naringenin to mitigate aseptic inflammatory pain.

Phagocytes such as macrophages and neutrophils express the NOX2 that has gp91<sup>phox</sup> as a subunit regulating superoxide anion production that, in turn, will lead to the production of other ROS and in the end lipid peroxidation [32].  $\text{TiO}_2$  enhances the phagocytic activity of neutrophils in a Syk (spleen tyrosine kinase)-dependent manner [64] and as a consequence activates NADPH oxidase generating superoxide anion [65]. Naringenin inhibited  $\text{TiO}_2$ -enhanced gp91<sup>phox</sup> mRNA expression, which corroborated the superoxide anion production and lipid peroxidation. In agreement, naringenin inhibits superoxide anion-induced oxidative stress inhibiting superoxide anion production, lipid peroxidation and gp91<sup>phox</sup> mRNA expression [14]. ROS contribute to tissue lesion and account for cartilage and bone destruction [66–69]. Superoxide anion causes bone fragility due to lowering the turnover resulting in osteoporosis and impairing collagen cross-linking [70]. For instance, ROS, and in specific gp91<sup>phox</sup>, contributes to osteoclast differentiation [71], and naringenin inhibits RANKL-induced osteoclast differentiation and bone resorption [20]. Superoxide anion

also induced hyperalgesia, edema, and leukocyte recruitment by further inducing the production of cytokines such as TNF $\alpha$  and IL-1 $\beta$  [14, 72], which were reduced by naringenin [14]. The superoxide anion-induced cytokine production depends on activating NF $\kappa$ B [72].

Herein, naringenin inhibited TiO<sub>2</sub>-induced mRNA expression of IL-33, TNF $\alpha$ , IL-1 $\beta$  and IL-6. TiO<sub>2</sub> activates macrophages [9], which release pro-inflammatory cytokines, including TNF $\alpha$  [9], IL-1 $\beta$  [73] and IL-6 [74]. Naringenin inhibits TNF $\alpha$ , IL-1 $\beta$ , IL-6 and IL-33 in carrageenan-, LPS-, and superoxide anion-induced inflammatory pain [14–16]. These cytokines participate in the chemoattraction of neutrophils [26, 40, 41]. TiO<sub>2</sub> also activates the recruited neutrophils [64] that participate in the destruction of cartilage and bone directly by releasing neutrophil extracellular traps (NETs). Releasing NETs results in histone citrullination, which is a mechanism involved in rheumatoid arthritis and also in TiO<sub>2</sub> and implant-induced arthritis [75]. Cytokines produced by TiO<sub>2</sub> stimulus, such as IL-33, IL-1 $\beta$ , and TNF $\alpha$  that increase the release of MMP, activate chondrocytes and osteoclasts [26, 76]. Further, naringenin inhibits IL-1 $\beta$ -induced MMP-3 production in primary cultured articular chondrocytes [55]. TNF $\alpha$  and IL-6 induce osteoclastogenesis in osteoclast medium culture with synovial cells from RANK knockout mice, showing a RANK-independent manner to induce osteoclast formation [30]. Naringenin might also inhibit osteoclast formation in a RANK-independent manner since it reduces TNF $\alpha$  and IL-6 production in LPS-induced inflammation [15]. TiO<sub>2</sub> also enhances neutrophils phagocytosis in a Syk (spleen tyrosine kinase)-dependent manner [64] and activates NADPH oxidase generating superoxide anion [65]. Cytokines produced upon TiO<sub>2</sub> stimulus induce superoxide anion production. This result lined up with the inhibition of leukocyte recruitment and also with the inhibition of oxidative stress, edema, cartilage destruction and bone degradation. In addition, evidence shows that naringenin reduces TNF $\alpha$ -induced ICAM-1 expression in human endothelial cells [77], a mechanism essential for leukocyte recruitment [78–80]. In chronic inflammation and neuropathic conditions IL-33 [33], TNF $\alpha$  [34], IL-1 $\beta$  [35] and IL-6 [36] activate sensory neurons, which is a nociceptive mechanism. In this sense, the inhibition of cytokine production is also an analgesic effect [81].

NF $\kappa$ B activation plays an essential role in the development and progression of arthritis once it is directly involved in the regulation of pro-inflammatory mediators production in the inflamed joint [82]. Herein, naringenin inhibited TiO<sub>2</sub>-induced NF $\kappa$ B activation in the knee joint. NF $\kappa$ B signaling pathway also possesses an important role in RANKL-induced osteoclast formation given that NF $\kappa$ B selective inhibitors such as SC-514 (IKK $\beta$  inhibitor) and NBD (IKK $\gamma$  inhibitor) block osteoclast differentiation [83]. Accumulated TiO<sub>2</sub> induces NF $\kappa$ B activation and

TNF $\alpha$  release in the brain of rats [84] and in HepG2 cells [85]. Further, naringenin inhibits NF $\kappa$ B activation in MIA-induced osteoarthritis [55] and in LPS- and carrageenan-induced inflammatory pain in mice [15, 16]. Therefore, naringenin inhibition of NF $\kappa$ B activation is a consistent effect in varied models.

In conclusion, the present data suggest that naringenin ameliorates TiO<sub>2</sub>-induced chronic arthritis. Naringenin mitigates TiO<sub>2</sub>-induced inflammatory pain, knee edema, histopathological damage, leukocyte recruitment, cartilage erosion, and bone resorption by inhibiting oxidative stress, cytokine mRNA expression, and NF $\kappa$ B activation. Therefore, naringenin represents a promising therapeutic approach to mitigate the complications related to implant-induced aseptic inflammation.

**Acknowledgements** We thank M.R.F.D.P., A.Z.Z., and M.M.B for the technical support and T.H.Z for the support in the Adobe Illustrator. This study was supported by grants from Conselho Nacional de Desenvolvimento Científico e Tecnológico (CNPq), São Paulo research Foundation (FAPESP) under grant agreements number 2011/19670-0 (Thematic project) and 2013/08216-2 (Center for Research in Inflammatory Disease-CRID), Coordenação de Aperfeiçoamento de Pessoal de Nível Superior (CAPES; Finance Code 001), and Programa de Pesquisa para o SUS (PPSUS) grant supported by Ministério da Ciência, Tecnologia e Inovação (MCTI), Secretaria da Ciência, Tecnologia e Ensino Superior (SETI), Decit/SCTIE/MS through CNPq with the support of Fundação Araucária and Secretaria da Saúde do Estado do Paraná (SESA-PR), and Parana State Government (Brazil).

## Compliance with ethical standards

**Conflict of interest** The authors declare no conflict of interest.

## References

1. Siddiqui MMA, Yeo SJ, Sivaiah P, Chia S-L, Chin PL, Lo NN. Function and quality of life in patients with recurvatum deformity after primary total knee arthroplasty: a review of our joint registry. *J Arthroplasty*. 2012;27(6):1106–10. <https://doi.org/10.1016/j.arth.2011.10.013>.
2. Soever LJ, Mackay C, Saryeddine T, Davis AM, Flannery JF, Jaglal SB, et al. Educational needs of patients undergoing total joint arthroplasty. *Physiother Can*. 2010;62(3):206–14. <https://doi.org/10.3138/physio.62.3.206>.
3. Maradit Kremers H, Larson DR, Crowson CS, Kremers WK, Washington RE, Steiner CA, et al. Prevalence of total hip and knee replacement in the United States. *J Bone Jt Surg Am*. 2015;97(17):1386–97. <https://doi.org/10.2106/JBJS.N.01141>.
4. Carr AJ, Robertsson O, Graves S, Price AJ, Arden NK, Judge A, et al. Knee replacement. *Lancet*. 2012;379(9823):1331–40. [https://doi.org/10.1016/S0140-6736\(11\)60752-6](https://doi.org/10.1016/S0140-6736(11)60752-6).
5. Cobelli N, Scharf B, Crisi GM, Hardin J, Santambrogio L. Mediators of the inflammatory response to joint replacement devices. *Nat Publ Group*. 2011;7(10):600–8. <https://doi.org/10.1038/nrrheum.2011.128>.
6. Goodman SB. Wear particles, periprosthetic osteolysis and the immune system. *Biomaterials*. 2007;28(34):5044–8. <https://doi.org/10.1016/j.biomaterials.2007.06.035>.

7. Gurr J-R, Wang ASS, Chen C-H, Jan K-Y. Ultrafine titanium dioxide particles in the absence of photoactivation can induce oxidative damage to human bronchial epithelial cells. *Toxicology*. 2005;213(1–2):66–73. <https://doi.org/10.1016/j.tox.2005.05.007>.
8. Apostu D, Lucaciu O, Lucaciu GDO, Crisan B, Crisan L, Baciut M, et al. Systemic drugs that influence titanium implant osseointegration. *Drug Metab Rev*. 2016;1–46. <https://doi.org/10.1080/03602532.2016.1277737>.
9. Dörner T, Haas J, Loddenkemper C, von Baehr V, Salama A. Implant-related inflammatory arthritis. *Nat Clin Pract Rheumatol*. 2006;2(1):53–6. <https://doi.org/10.1038/ncprheum0087>.
10. Borghi SM, Mizokami SS, Pinho-Ribeiro FA, Fattori V, Crespigo J, Clemente-Napimoga JT, et al. The flavonoid quercetin inhibits titanium dioxide (TiO<sub>2</sub>)-induced chronic arthritis in mice. *J Nutr Biochem*. 2017;53:81–95. <https://doi.org/10.1016/j.jnutbio.2017.10.010>.
11. Verri WA, Vicentini FTMC, Baracat MM, Georgetti SR, Cardoso RDR, Cunha TM, et al. Flavonoids as anti-inflammatory and analgesic drugs: mechanisms of action and perspectives in the development of pharmaceutical forms. In: Atta-ur-Rahman, editor. *Studies in Natural Products Chemistry*; 2012. pp. 297–330.
12. Lee CH, Jeong TS, Choi YK, Hyun BH, Oh GT, Kim EH, et al. Anti-atherogenic effect of citrus flavonoids, naringin and naringenin, associated with hepatic ACAT and aortic VCAM-1 and MCP-1 in high cholesterol-fed rabbits. *Biochem Biophys Res Commun*. 2001;284(3):681–8. <https://doi.org/10.1006/bbrc.2001.5001>.
13. Sun H, Dong T, Zhang A, Yang J, Yan G, Sakurai T, et al. Pharmacokinetics of hesperetin and naringenin in the Zhi Zhu Wan, a traditional Chinese medicinal formulae, and its pharmacodynamics study. *Phytother Res*. 2013;27(9):1345–51. <https://doi.org/10.1002/ptr.4867>.
14. Manchope MF, Calixto-Campos C, Coelho-Silva L, Zarpelon AC, Pinho-Ribeiro FA, Georgetti SR, et al. Naringenin inhibits superoxide anion-induced inflammatory pain: role of oxidative stress, cytokines, Nrf-2 and the NO-cGMP-PKG-KATP channel signaling pathway. *PLoS One*. 2016;11(4):e0153015-e. <https://doi.org/10.1371/journal.pone.0153015>.
15. Pinho-Ribeiro FA, Zarpelon AC, Mizokami SS, Borghi SM, Bordignon J, Silva RL, et al. The citrus flavonone naringenin reduces lipopolysaccharide-induced inflammatory pain and leukocyte recruitment by inhibiting NF-κB activation. *J Nutr Biochem*. 2016;33:8–14. <https://doi.org/10.1016/j.jnutbio.2016.03.013>.
16. Pinho-Ribeiro FA, Zarpelon AC, Fattori V, Manchope MF, Mizokami SS, Casagrande R, et al. Naringenin reduces inflammatory pain in mice. *Neuropharmacology*. 2016;105:508–19. <https://doi.org/10.1016/j.neuropharm.2016.02.019>.
17. Wang J, Fan Y. Lung injury induced by TiO<sub>2</sub> nanoparticles depends on their structural features: Size, shape, crystal phases, and surface coating. *Int J Mol Sci*. 2014;15(12):22258–78. <https://doi.org/10.3390/ijms151222258>.
18. Ashley NT, Weil ZM, Nelson RJ. Inflammation: mechanisms, costs, and natural variation. *Annu Rev Ecol Syst*. 2012;43:385–406. <https://doi.org/10.1146/annurev-ecolsys-040212-092530>.
19. Smolen JS, Aletaha D, McInnes IB. Rheumatoid arthritis. *Lancet*. 2016;388(10055):2023–38. [https://doi.org/10.1016/S0140-6736\(16\)30173-8](https://doi.org/10.1016/S0140-6736(16)30173-8).
20. Wang W, Wu C, Tian B, Liu X, Zhai Z, Qu X, et al. The inhibition of RANKL-induced osteoclastogenesis through the suppression of p38 signaling pathway by naringenin and attenuation of titanium-particle-induced osteolysis. *Int J Mol Sci*. 2014;15(12):21913–34. <https://doi.org/10.3390/ijms151221913>.
21. Wang JX, Fan YB, Gao Y, Hu QH, Wang TC. TiO<sub>2</sub> nanoparticles translocation and potential toxicological effect in rats after intraarticular injection. *Biomaterials*. 2009;30(27):4590–600. <https://doi.org/10.1016/j.biomaterials.2009.05.008>.
22. Guerrero ATG, Verri WA, Cunha TM, Silva TA, Rocha FAC, Ferreira SH, et al. Hypernociception elicited by tibio-tarsal joint flexion in mice: a novel experimental arthritis model for pharmacological screening. *Pharmacol Biochem Behav*. 2006;84(2):244–51. <https://doi.org/10.1016/j.pbb.2006.05.008>.
23. Yamanaka H, Goto K, Miyamoto K. Scoring evaluation for histopathological features of synovium in patients with rheumatoid arthritis during anti-tumor necrosis factor therapy. *Rheumatol Int*. 2010;30(3):409–13. <https://doi.org/10.1007/s00296-009-1158-2>.
24. Sun J, Hua B, Livingston EW, Taves S, Johansen PB, Hoffman M, et al. Abnormal joint and bone wound healing in hemophilia mice is improved by extending factor IX activity after hemarthrosis. *Blood*. 2017;129(15):2161–71. <https://doi.org/10.1182/blood-2016-08-734053>.
25. Casagrande R, Georgetti SR, Verri WA, Dorta DJ, dos Santos AC, Fonseca MJV. Protective effect of topical formulations containing quercetin against UVB-induced oxidative stress in hairless mice. *J Photochem Photobiol B Biol*. 2006;84(1):21–7. <https://doi.org/10.1016/j.jphotobiol.2006.01.006>.
26. Verri WA, Souto FO, Vieira SM, Almeida SCL, Fukada SY, Xu D, et al. IL-33 induces neutrophil migration in rheumatoid arthritis and is a target of anti-TNF therapy. *Ann Rheum Dis*. 2010;69(9):1697–703. <https://doi.org/10.1136/ard.2009.122655>.
27. Vieira SM, Cunha TM, Franca RF, Pinto LG, Talbot J, Turato WM, et al. Joint NOD2/RIPK2 signaling regulates IL-17 axis and contributes to the development of experimental arthritis. *J Immunol*. 2012;188(10):5116–22. <https://doi.org/10.4049/jimmunol.1004190>.
28. Hohmann MSN, Cardoso RDR, Pinho-Ribeiro FA, Crespigo J, Cunha TM, Alves-Filho JC, et al. 5-lipoxygenase deficiency reduces acetaminophen-induced hepatotoxicity and lethality. *BioMed Res Int*. 2013;2013:627046-. <https://doi.org/10.1155/2013/627046>.
29. Guedes RP, Bosco LD, Teixeira CM, Araújo ASR, Llesuy S, Belló-Klein A, et al. Neurothematic pain modifies antioxidant activity in rat spinal cord. *Neurochem Res*. 2006;31(5):603–9. <https://doi.org/10.1007/s11064-006-9058-2>.
30. O'Brien W, Fissel BM, Maeda Y, Yan J, Ge X, Gravalles EM, et al. RANK-independent osteoclast formation and bone erosion in inflammatory arthritis. *Arthritis Rheumatol*. 2016;68(12):2889–900. <https://doi.org/10.1002/art.39837>.
31. Danks L, Komatsu N, Guerrini MM, Sawa S, Armaka M, Kollias G, et al. RANKL expressed on synovial fibroblasts is primarily responsible for bone erosions during joint inflammation. *Ann Rheum Dis*. 2016;75(6):1187–95. <https://doi.org/10.1136/annrheumdis-2014-207137>.
32. Lambeth JD. NOX enzymes and the biology of reactive oxygen. *Nat Rev Immunol*. 2004;4(3):181–9. <https://doi.org/10.1038/nri1312>.
33. Liu B, Tai Y, Achanta S, Kaelberer MM, Caceres AI, Shao X, et al. IL-33/ST2 signaling excites sensory neurons and mediates itch response in a mouse model of poison ivy contact allergy. *Proc Natl Acad Sci*. 2016;113(47):E7572–9. <https://doi.org/10.1073/pnas.1606608113>.
34. Jin X, Gereau RW. Acute p38-mediated modulation of tetrodotoxin-resistant sodium channels in mouse sensory neurons by tumor necrosis factor. *J Neurosci*. 2006;26(1):246–55. <https://doi.org/10.1523/JNEUROSCI.3858-05.2006>.
35. Binshtok AM, Wang H, Zimmermann K, Amaya F, Vardeh D, Shi L, et al. Nociceptors are interleukin-1 sensors. *J Neurosci*. 2008;28(52):14062–73. <https://doi.org/10.1523/JNEUROSCI.3795-08.2008>.
36. Ebbinghaus M, Segond von Banchet G, Massier J, Gajda M, Brauer R, Kress M, et al. Interleukin-6-dependent influence

- of nociceptive sensory neurons on antigen-induced arthritis. *Arthritis Res Ther*. 2015;17:334. <https://doi.org/10.1186/s13075-015-0858-0>.
37. Vieira SM, Lemos HP, Grespan R, Napimoga MH, Dal-Secco D, Freitas A, et al. A crucial role for TNF-alpha in mediating neutrophil influx induced by endogenously generated or exogenous chemokines, KC/CXCL1 and LIX/CXCL5. *Br J Pharmacol*. 2009;158(3):779–89. <https://doi.org/10.1111/j.1476-5381.2009.00367.x>.
  38. Mascarenhas DP, Pereira MS, Manin GZ, Hori JI, Zamboni DS. Interleukin 1 receptor-driven neutrophil recruitment accounts to MyD88-dependent pulmonary clearance of legionella pneumophila infection in vivo. *J Infect Dis*. 2015;211(2):322–30. <https://doi.org/10.1093/infdis/jiu430>.
  39. Romano M, Sironi M, Toniatti C, Polentarutti N, Fruscella P, Ghezzi P, et al. Role of IL-6 and its soluble receptor in induction of chemokines and leukocyte recruitment. *Immunity*. 1997;6(3):315–25.
  40. Lan F, Yuan B, Liu T, Luo X, Huang P, Liu Y, et al. Interleukin-33 facilitates neutrophil recruitment and bacterial clearance in *S. aureus*-caused peritonitis. *Mol Immunol*. 2016;72:74–80. <https://doi.org/10.1016/j.molimm.2016.03.004>.
  41. Alves-Filho JC, Sonogo F, Souto FO, Freitas A, Verri WA Jr, Auxiliadora-Martins M, et al. Interleukin-33 attenuates sepsis by enhancing neutrophil influx to the site of infection. *Nat Med*. 2010;16(6):708–12. <https://doi.org/10.1038/nm.2156>.
  42. Poynter ME, Irvin CG, Janssen-Heininger YM. A prominent role for airway epithelial NF-kappa B activation in lipopolysaccharide-induced airway inflammation. *J Immunol*. 2003;170(12):6257–65.
  43. Anrather J, Racchumi G, Iadecola C. NF-kappaB regulates phagocytic NADPH oxidase by inducing the expression of gp91phox. *J Biol Chem*. 2006;281(9):5657–67. <https://doi.org/10.1074/jbc.M506172200>.
  44. Harris WH. Wear and periprosthetic osteolysis the problem. *Clin Orthop Relat Res*. 2001(393):66–70.
  45. Long M, Rack HJ. Titanium alloys in total joint replacement—a materials science perspective. *Biomaterials*. 1998;19(18):1621–39.
  46. Chobot V, Hadacek F. Exploration of pro-oxidant and antioxidant activities of the flavonoid myricetin. *Redox Rep*. 2011;16(6):242–7. <https://doi.org/10.1179/1351000211Y.0000000015>.
  47. Straub I, Mohr F, Stab J, Konrad M, Philipp SE, Oberwinkler J, et al. Citrus fruit and fabacea secondary metabolites potently and selectively block TRPM3. *Br J Pharmacol*. 2013;168(8):1835–50. <https://doi.org/10.1111/bph.12076>.
  48. Manchope MF, Casagrande R, Verri JWA, Manchope MF, Casagrande R, Verri JWA. Naringenin: an analgesic and anti-inflammatory citrus flavanone. *Oncotarget*. 2017;8(3):3766–7. <https://doi.org/10.18632/oncotarget.14084>.
  49. Murakawa M, Yamaoka K, Tanaka Y, Fukuda Y. Involvement of tumor necrosis factor (TNF)-alpha in phorbol ester 12-*O*-tetradecanoylphorbol-13-acetate (TPA)-induced skin edema in mice. *Biochem Pharmacol*. 2006;71(9):1331–6. <https://doi.org/10.1016/j.bcp.2006.01.005>.
  50. Seven A, Guzel S, Seymen O, Civelek S, Bolayirli M, Yigit G, et al. Nitric oxide synthase inhibition by L-NAME in streptozotocin induced diabetic rats: impacts on oxidative stress. *Tohoku J Exp Med*. 2003;199(4):205–10.
  51. Salvemini D, Wang ZQ, Wyatt PS, Bourdon DM, Marino MH, Manning PT, et al. Nitric oxide: a key mediator in the early and late phase of carrageenan-induced rat paw inflammation. *Br J Pharmacol*. 1996;118(4):829–38.
  52. Fattori V, Amaral FA, Verri WA. Neutrophils and arthritis: role in disease and pharmacological perspectives. *Pharmacol Res*. 2016. <https://doi.org/10.1016/j.phrs.2016.01.027>.
  53. Scott DL, Wolfe F, Huizinga TWJ. Rheumatoid arthritis. *Lancet*. 2010;376(9746):1094–108. [https://doi.org/10.1016/S0140-6736\(10\)60826-4](https://doi.org/10.1016/S0140-6736(10)60826-4).
  54. Kongpichitchoke T, Hsu J-L, Huang T-C. Number of hydroxyl groups on the B-Ring of flavonoids affects their antioxidant activity and interaction with phorbol ester binding site of PKCδ C1B domain: in vitro and in silico studies. *J Agric Food Chem*. 2015;63(18):4580–6. <https://doi.org/10.1021/acs.jafc.5b00312>.
  55. Wang CC, Guo L, Tian FD, An N, Luo L, Hao RH, et al. Naringenin regulates production of matrix metalloproteinases in the knee-joint and primary cultured articular chondrocytes and alleviates pain in rat osteoarthritis model. *Braz J Med Biol Res*. 2017;50(4):e5714. <https://doi.org/10.1590/1414-431X20165714>.
  56. Murphy G, Lee MH. What are the roles of metalloproteinases in cartilage and bone damage? *Ann Rheum Dis*. 2005;64(Suppl 4):iv44–7. <https://doi.org/10.1136/ard.2005.042465>.
  57. Lin PM, Chen CT, Torzilli PA. Increased stromelysin-1 (MMP-3), proteoglycan degradation (3B3- and 7D4) and collagen damage in cyclically load-injured articular cartilage. *Osteoarthritis Cartilage*. 2004;12(6):485–96. <https://doi.org/10.1016/j.joca.2004.02.012>.
  58. Steinert AF, Noth U, Tuan RS. Concepts in gene therapy for cartilage repair. *Injury*. 2008;39(Suppl 1):97–113. <https://doi.org/10.1016/j.injury.2008.01.034>.
  59. Hofbauer LC, Schoppet M. Clinical implications of the osteoprotegerin/RANKL/RANK system for bone and vascular diseases. *JAMA*. 2004;292(4):490–. <https://doi.org/10.1001/jama.292.4.490>.
  60. Boyle WJ, Simonet WS, Lacey DL. Osteoclast differentiation and activation. *Nature*. 2003;423(6937):337–42. <https://doi.org/10.1038/nature01658>.
  61. Chakravarti A, Raquil M-A, Tessier P, Poubelle PE. Surface RANKL of Toll-like receptor 4–stimulated human neutrophils activates osteoclastic bone resorption. *Blood*. 2009;114(8).
  62. Al-Rejaie SS, Aleisa AM, Abuhashish HM, Parmar MY, Ola MS, Al-Hosaini AA, et al. Naringenin neutralises oxidative stress and nerve growth factor discrepancy in experimental diabetic neuropathy. *Neurol Res*. 2015;37(10):924–33. <https://doi.org/10.1179/1743132815Y.0000000079>.
  63. Nishimura FdCY, de Almeida AC, Ratti BA, Ueda-Nakamura T, Nakamura CV, Ximenes VF, et al. Antioxidant effects of quercetin and naringenin are associated with impaired neutrophil microbicidal activity. *Evid Based Complement Alternat Med*. 2013;2013:795916-. <https://doi.org/10.1155/2013/795916>.
  64. Gonçalves DM, Chiasson S, Girard D. Activation of human neutrophils by titanium dioxide (TiO<sub>2</sub>) nanoparticles. *Toxicol In Vitro*. 2010;24(3):1002–8. <https://doi.org/10.1016/j.tiv.2009.12.007>.
  65. Masoud R, Bizouarn T, Trepout S, Wien F, Baciou L, Marco S, et al. Titanium dioxide nanoparticles increase superoxide anion production by acting on NADPH oxidase. *PLoS One*. 2015;10(12):e0144829-e. <https://doi.org/10.1371/journal.pone.0144829>.
  66. Callaway DA, Jiang JX. Reactive oxygen species and oxidative stress in osteoclastogenesis, skeletal aging and bone diseases. *J Bone Miner Metab*. 2015;33(4):359–70. <https://doi.org/10.1007/s00774-015-0656-4>.
  67. Kim MS, Yang YM, Son A, Tian YS, Lee SI, Kang SW, et al. RANKL-mediated reactive oxygen species pathway that induces long lasting Ca<sup>2+</sup> oscillations essential for osteoclastogenesis. *J Biol Chem*. 2010;285(10):6913–21. <https://doi.org/10.1074/jbc.M109.051557>.
  68. Rees MD, Hawkins CL, Davies MJ. Hypochlorite and superoxide radicals can act synergistically to induce fragmentation of hyaluronan and chondroitin sulphates. *Biochem J*. 2004;381(Pt 1):175–84. <https://doi.org/10.1042/BJ20040148>.

69. Henrotin YE, Bruckner P, Pujol JP. The role of reactive oxygen species in homeostasis and degradation of cartilage. *Osteoarthritis Cartilage*. 2003;11(10):747–55.
70. Nojiri H, Saita Y, Morikawa D, Kobayashi K, Tsuda C, Miyazaki T, et al. Cytoplasmic superoxide causes bone fragility owing to low-turnover osteoporosis and impaired collagen cross-linking. *J Bone Miner Res*. 2011;26(11):2682–94. <https://doi.org/10.1002/jbmr.489>.
71. Kang IS, Kim C. NADPH oxidase gp91(phox) contributes to RANKL-induced osteoclast differentiation by upregulating NFATc1. *Sci Rep*. 2016;6:38014. <https://doi.org/10.1038/srep38014>.
72. Pinho-Ribeiro FA, Fattori V, Zarpelon AC, Borghi SM, Staurengo-Ferrari L, Carvalho TT, et al. Pyrrolidine dithiocarbamate inhibits superoxide anion-induced pain and inflammation in the paw skin and spinal cord by targeting NF- $\kappa$ B and oxidative stress. *Inflammopharmacology*. 2016;24(2–3):97–107. <https://doi.org/10.1007/s10787-016-0266-3>.
73. St Pierre CA, Chan M, Iwakura Y, Ayers DC, Kurt-Jones EA, Finberg RW. Periprosthetic osteolysis: characterizing the innate immune response to titanium wear-particles. *J Orthop Res*. 2010;28(11):1418–24. <https://doi.org/10.1002/jor.21149>.
74. Borgognoni CF, Mormann M, Qu Y, Schäfer M, Langer K, Öztürk C, et al. Reaction of human macrophages on protein corona covered TiO<sub>2</sub> nanoparticles. *Nanomedicine: nanotechnology, biology, and medicine*. 2015;11(2):275–82. <https://doi.org/10.1016/j.nano.2014.10.001>.
75. Vitkov L, Krautgartner W-D, Obermayer A, Stoiber W, Hanig M, Klappacher M, et al. The initial inflammatory response to bioactive implants is characterized by NETosis. *PLoS One*. 2015;10(3):e0121359-e. <https://doi.org/10.1371/journal.pone.0121359>.
76. Wright HL, Moots RJ, Edwards SW. The multifactorial role of neutrophils in rheumatoid arthritis. *Nat Rev Rheumatol*. 2014;10(10):593–601. <https://doi.org/10.1038/nrrheum.2014.80>.
77. Freischmidt A, Jürgenliemk G, Kraus B, Okpanyi SN, Müller J, Kelber O, et al. Contribution of flavonoids and catechol to the reduction of ICAM-1 expression in endothelial cells by a standardised Willow bark extract. *Phytomedicine*. 2012;19(3–4):245–52. <https://doi.org/10.1016/j.phymed.2011.08.065>.
78. Martinelli R, Gegg M, Longbottom R, Adamson P, Turowski P, Greenwood J. ICAM-1-mediated endothelial nitric oxide synthase activation via calcium and AMP-activated protein kinase is required for transendothelial lymphocyte migration. *Mol Biol Cell*. 2009;20(3):995–1005. <https://doi.org/10.1091/mbc.E08-06-0636>.
79. Dal Secco D, Moreira AP, Freitas A, Silva JS, Rossi MA, Ferreira SH, et al. Nitric oxide inhibits neutrophil migration by a mechanism dependent on ICAM-1: role of soluble guanylate cyclase. *Nitric Oxide*. 2006;15(1):77–86. <https://doi.org/10.1016/j.niox.2006.02.004>.
80. Kevil CG, Patel RP, Bullard DC. Essential role of ICAM-1 in mediating monocyte adhesion to aortic endothelial cells. *Am J Physiol Cell Physiol*. 2001;281(5):C1442–7.
81. Verri WA, Cunha TM, Parada CA, Poole S, Cunha FQ, Ferreira SH. Hypernociceptive role of cytokines and chemokines: targets for analgesic drug development? *Pharmacol Ther*. 2006;112(1):116–38. <https://doi.org/10.1016/j.pharmthera.2006.04.001>.
82. Simmonds RE, Foxwell BM. Signalling, inflammation and arthritis: NF- $\kappa$ B and its relevance to arthritis and inflammation. *Rheumatology*. 2008;47(5):584–90. <https://doi.org/10.1093/rheumatology/kem298>.
83. Yu M, Qi X, Moreno JL, Farber DL, Keegan AD. NF- $\kappa$ B signaling participates in both RANKL- and IL-4-induced macrophage fusion: receptor cross-talk leads to alterations in NF- $\kappa$ B pathways. *J Immunol*. 2011;187(4):1797–806. <https://doi.org/10.4049/jimmunol.1002628>.
84. Meena R, Kumar S, Paulraj R. Titanium oxide (TiO<sub>2</sub>) nanoparticles in induction of apoptosis and inflammatory response in brain. *J Nanopart Res*. 2015;17(1):49-. <https://doi.org/10.1007/s11051-015-2868-x>.
85. Prasad RY, Simmons SO, Killius MG, Zucker RM, Kligerman AD, Blackman CF, et al. Cellular interactions and biological responses to titanium dioxide nanoparticles in HepG2 and BEAS-2B cells: role of cell culture media. *Environ Mol Mutagen*. 2014;55(4):336–42. <https://doi.org/10.1002/em.21848>.